

# Dislocation and Temperature Effects on Zero-Bias Resistance-Area Product of InGaSb PIN Photodiodes

Mehbuba Tanzid\*, Farseem M. Mohammedy  
Department of Electrical & Electronic Engineering  
Bangladesh University of Engineering & Technology (BUET)  
Dhaka, Bangladesh  
E-mail address: \*mihika193@gmail.com

**Abstract**—The effects of dislocation and temperature on zero-bias resistance-area product ( $R_0A$ ) of InGaSb PIN photodiodes are analyzed using a model which takes into account the dislocation and temperature dependence of minority carrier lifetime and the effect of space charge density around the dislocation core. Dislocation tends to decrease the zero-bias resistance-area product by adding shunt impedance paths for dark current flow as well as by reducing the minority carrier lifetime. Through the dislocation and temperature dependant modeling, maximum  $R_0A$  is found to be  $1.85 \Omega \text{ cm}^2$  at 139 K for InGaSb PIN photodiodes. Theoretical results are fitted with experimental data obtained at 300 K and 363 K.

**Keywords**— $R_0A$  product; Dislocation; InGaSb; PIN photodiode; Surface leakage.

## I. INTRODUCTION

GaSb and related materials has achieved growing interest in recent times for potential new device applications originating from their excellent optical and electronic properties. One particular GaSb-based easy-to-grow ternary is InGaSb which is finding ever increasing applications as photodetectors and lasers operating adequately well in the 1.7-6.9 $\mu\text{m}$  wavelength range, and which has interesting biomedical and security applications. One specific example is the use of InGaSb-based photodetectors in remote sensing of biotoxins. [1]

In order to tune the device to a specific wavelength, it is necessary to use ternary InGaSb with composition appropriate to the desired wavelength. InGaSb has lattice constant different to the GaSb substrate resulting in strained growth and high defect densities. In order to mitigate this problem, metamorphic buffer layers (M-buffers) are used allowing growth of a new pseudo-substrate having the desired lattice constant on which to grow the device structure with low defect densities. Metamorphic buffers allow for the growth of layers of materials with a desired lattice constant on a substrate of a different lattice constant. The lattice mismatches in the buffers are accommodated through the formation of dislocations. So it is necessary to take into account the effect of dislocations in the material while characterizing different electrical and optical parameters of such metamorphically grown photodiodes. The effect of dislocations has been analyzed for mercury cadmium telluride (HgCdTe) photodiodes in [2]-[5].

It has been shown that dislocations, besides operating as a shunt, also influence the diode impedance through their effect on minority carrier lifetime. In addition to the dislocation dependence, the temperature dependence of minority carrier lifetime is also included in the model described for mercury cadmium telluride (HgCdTe) photovoltaic detectors in [5]. An analysis of leakage current for GaInAsSb photodiodes has been done in [6] and a temperature dependent model of minority carrier lifetime, especially for InGaSb, has been depicted in [7]. But dislocation effect is yet to be included in the models for InGaSb PIN photodiodes.

For the present work, step-graded metamorphic layers of  $\text{In}_x\text{Ga}_{1-x}\text{Sb}$  on GaSb with terminating composition  $x=0.15$  have been grown. PIN diodes of various sizes have been successfully regrown on one of those samples having low dislocations with satisfactory dark current characteristics. A complete experimental detail is depicted in [8],[9]. In this paper, the effects of dislocation and temperature on zero-bias resistance-area product ( $R_0A$ ) of InGaSb PIN photodiodes are analyzed using a model which takes into account the dislocation and temperature dependence of minority carrier lifetime and the effect of space charge density around the dislocation core.

## II. THEORETICAL MODEL

The device schematic used for the theoretical modeling and calculation is shown in Fig. 1. An n-i-p mesa diode structure has been considered throughout the modeling. The values used for various physical parameters are listed in Table I.

### A. Minority Carrier Lifetime

To include temperature dependence in the minority carrier lifetime of InGaSb, the model described in [7] is adapted. The model takes into account various recombination mechanisms such as the nonradiative Shockley-Read-Hall ( $\tau_{SRH}$ ) and Auger recombination lifetimes ( $\tau_{Auger}$ ). The total minority carrier lifetime is obtained from the inverse of the sum of their reciprocals. For example, in the case of minority carrier life time for electron the expression is

$$\tau_{n0} = \left( \frac{1}{\tau_{SRH}} + \frac{1}{\tau_{Auger}} \right)^{-1} \quad (1)$$

The nonradiative Shockley-Read-Hall ( $\tau_{SRH}$ ) lifetime is given by [7],

$$\tau_{SRH} = \frac{1}{\sigma \cdot N_t} \sqrt{\frac{m_0}{3kT}}, \quad (2)$$

where  $\sigma$  is the capture cross section of minority carriers,  $N_t$  is the density of traps,  $T$  is temperature and  $k$  is the Boltzmann constant.

TABLE I. PARAMETERS USED

| Parameter                                   | Value (Unit)                                    | Ref.    | Parameter | Value (Unit)                                  | Ref. |
|---|---|---------|-----------|---|------|
| $\text{In}_x\text{Ga}_{1-x}\text{Sb}$ , $x$ | 0.107   | [8]     | $N_A$     | $2 \times 10^{18} \text{ cm}^{-3}$            | [8]  |
| $C_B$                                       | 0.415eV   | [7],[8] | $N_D$     | $1.5 \times 10^{18} \text{ cm}^{-3}$          | [8]  |
| $\delta$                                    | $0.000406621 \text{ eVK}^{-1}$                  | [7],[8] | $N_t$     | $2.4 \times 10^{16} \text{ cm}^{-3}$          | [8]  |
| $\beta$                                     | 143.21K   | [7],[8] | $N_t$     | $2.8 \times 10^{13} \text{ cm}^{-3}$          | [8]  |
| $\Delta_0$                                  | 0.8eV   | [7],[8] | $E_t$     | $E_v+0.1\text{eV}$<br>$E_v+0.3\text{eV}$      | [13] |
| $m_0$                                       | $9.109 \times 10^{-31} \text{ kg}$              | -       | $\sigma$  | $1.5 \times 10^{-19} \text{ m}^2$             | [7]  |
| $m_e/m_0$                                   | 0.03723   | [8]     | $a$       | 6.14Å   | [8]  |
| $m_h/m_0$                                   | 0.29391   | [8]     | $N$       | $6.67 \times 10^8 \text{ cm}^{-2}$            | [10] |
| $m_s/m_0$                                   | 0.11893   | [8]     | $\mu_n$   | $2164 \text{ cm}^2\text{V}^{-1}\text{s}^{-1}$ | [8]  |
| $K_n$                                       | $3 \times 10^{-20} \text{ cm}^3\text{s}^{-1}$   | [1]     | $\mu_p$   | $468 \text{ cm}^2\text{V}^{-1}\text{s}^{-1}$  | [8]  |
| $K_p$                                       | $7.1 \times 10^{-20} \text{ cm}^3\text{s}^{-1}$ | [1]     | $S_n$     | $225.84 \text{ cms}^{-1}$                     | [10] |

For  $\text{In}_{0.107}\text{Ga}_{0.893}\text{Sb}$ , three significant Auger recombination mechanisms are between the conduction/valence bands (A-1), through the conduction/heavy-hole/light-hole bands (CHLH or A-7) and conduction/heavy-hole/spin split-off bands (CHSH or A-S). Thus, the total Auger lifetime can be expressed as,

$$\frac{1}{\tau_{Auger}} = \frac{(n_{p0} + p_{p0})}{2} \left[ \frac{1}{P_{p0}\tau_{A1}} + \frac{1}{n_{p0}\tau_{A7}} + \frac{1}{n_{p0}\tau_{AS}} \right]. \quad (3)$$

where  $n_{p0}$  and  $p_{p0}$  are the equilibrium electron and hole concentration in p-type material, respectively.  $\tau_{A1}$ ,  $\tau_{A7}$  and  $\tau_{AS}$  are intrinsic lifetimes for the previously mentioned three Auger mechanisms and their expressions are same as those given in [7].

To include the dislocation effect in the minority carrier lifetime of electrons the expression is given as [4],

$$\frac{1}{\tau_n} = \frac{1}{\tau_{n0}} + 2\pi masN, \quad (4)$$

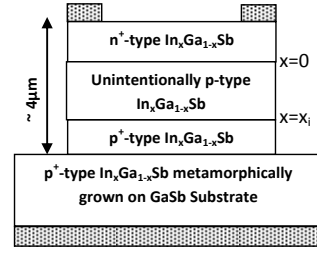


Figure 1. Device schematic structure.

where  $m$  is an integer with minimum value of unity,  $a$  is lattice constant of  $\text{In}_x\text{Ga}_{1-x}\text{Sb}$ ,  $s$  is surface recombination velocity and  $N$  is dislocation density. Similar expressions as in (1) to (4) can be written for minority carrier lifetime of hole,  $\tau_{p0}$  and  $\tau_p$ , by using appropriate parameters for hole.

### B. Surface Recombination Velocity

By treating discontinuity in the lattice at each dislocation equivalent to the discontinuity of the lattice at a planar surface, the magnitude of the recombination velocity may be estimated in a way similar to the calculation of the recombination velocity at the surface of a semiconductor wafer [3]. Thus the expression for recombination velocity at each dislocation is

$$s = \frac{\sqrt{K_n K_p} (n_0 + p_0)}{2n_i \{ \cosh[(E_t - E_i)/kT - u_0] + \cosh(qU_s/kT - u_0) \}}, \quad (5)$$

where  $K_n$  and  $K_p$  are the capture probabilities for electrons and holes, respectively, by the surface states [1].  $n_0$  and  $p_0$  are the electron and hole densities in the bulk, away from the dislocations.  $E_t$  is the trap energy level,  $E_i$  is the intrinsic Fermi level in the bulk and  $u_0 = 0.5 \ln(K_p/K_n)$ .

The potential at the surface of the core of the dislocation,  $U_s$ , can be determined by the following equations [4]:

$$Q_{SC} = q(n_0 + p_0)L_{db} F_t, \quad (6)$$

$$F_t = \sqrt{2} \left\{ \frac{\cosh(u_b + v_s)}{\cosh u_b} - v_s \tanh u_b - 1 + \frac{N_t}{(n_0 + p_0)} \times \left[ \ln \left( 1 + \frac{\exp v_s}{1 + \exp(E_t/kT)} \right) - \frac{v_s}{1 + \exp(E_t/kT)} \right] \right\}^{1/2}, \quad (7)$$

where  $Q_{SC}$  is space charge density,  $L_{db}$  is effective Debye length,  $U_b$  is the bulk potential, and the reduced potentials,  $u_s = qU_s/kT$  and  $v_s = q(U_s - U_b)/kT$ .

### C. Zero-Bias Resistance-Area Product

The model for HgCdTe considered semi-infinite base by assuming much smaller minority carrier diffusion length. By assuming that the thickness of n and p regions of the diode is much smaller than the minority carrier diffusion lengths, the zero-bias resistance area product model for the current mesa diode is given by [10],

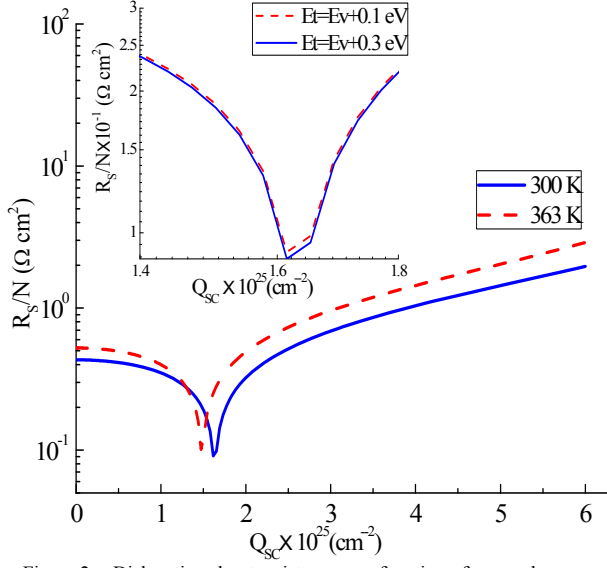


Figure 2. Dislocation shunt resistance as a function of space charge density and temperature.

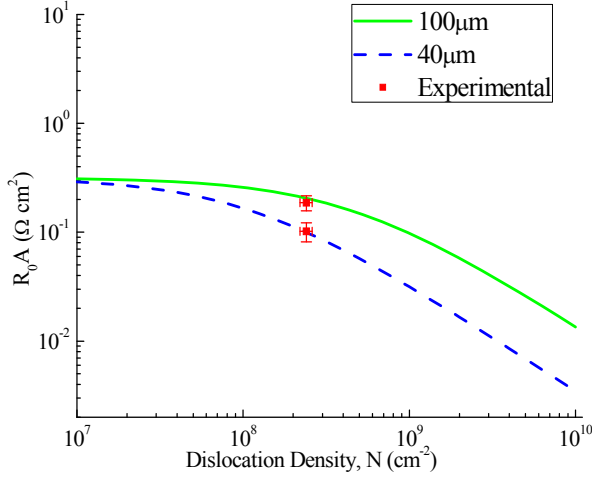


Figure 3. Zero-bias resistance-area product ( $R_0A$ ) a function of dislocation density and device dimension.

$$\frac{1}{R_0A} = \frac{(L_n - x_p)^2}{4} \left( \frac{1}{(R_0A_S)_S} \right) \left( \frac{p}{A} \right)^2 + L_n \left( \frac{1}{(R_0A_S)_S} \right) \left( \frac{p}{A} \right) + \left( \frac{1}{R_{DA_j}} + \frac{1}{(R_0A)_{g-r}} \right) \quad (8)$$

where  $(R_0A_S)_S$  is the surface leakage component,  $R_{DA_j}$  is the bulk diffusion and  $(R_0A)_{g-r}$  is the component from recombination at the bulk space charge region of the diode.  $L_n$  is the minority carrier diffusion length for the p-side of the diode,  $x_p$  is the thickness of mesa exposed p-region of the diode,  $p$  is perimeter and  $A$  is area of the diode.

The diffusion component is affected by the recombination of minority carriers at the undoped InGaSb and p<sup>+</sup>-InGaSb interface where there is a concentration gradient of carriers giving rise to a surface recombination velocity. The expression is given by [7],

$$\frac{1}{R_{DA_j}} = \frac{q^2 n_i^2}{kT} \left\{ \frac{L_p}{\tau_p N_D} + \frac{L_n}{\tau_n N_I} \left[ \frac{\left( \frac{S_n}{D_n} \frac{1}{L_n} \right) e^{\frac{x_i}{L_n}} - \left( \frac{S_n + 1}{D_n + L_n} \right) e^{-\frac{x_i}{L_n}}}{\left( \frac{S_n}{D_n} \frac{1}{L_n} \right) e^{\frac{x_i}{L_n}} + \left( \frac{S_n + 1}{D_n + L_n} \right) e^{-\frac{x_i}{L_n}}} \right] \right\} \quad (9)$$

where  $S_n$  is the surface recombination velocity and  $x_i$  is the position of i-InGaSb/p-InGaSb interface,  $N_I$  and  $N_D$  are the doping densities in undoped and n region, respectively, and  $D_p$  and  $D_n$  are the minority carrier diffusion constants in the p and n-type material, respectively. The diffusion constants are obtained from experimental carrier mobilities,  $\mu_p$  and  $\mu_n$ , using the Einstein relation,  $D/\mu = kT/q$ . The zero-bias resistance area product from generation-recombination at the bulk region of the diode is given by [6],

$$(R_0A)_{g-r} = \frac{\tau_p V_{bi}}{qn_i W} \quad (10)$$

where  $V_{bi}$  is the built-in potential and  $W$  is the depletion layer width. The contribution from surface leakage to the zero-bias resistance can be expressed as [4],

$$R_S = \frac{kT}{2\pi q^2 n_i s_{mat}} \quad (11)$$

$$(R_0A_S)_S = \frac{R_S \times A_S}{N} \quad (12)$$

where  $R_S$  is the contribution from each individual dislocation. The area  $A_S$  can be written as irrespective of square or circular mesa sample [11],

$$A_S = \frac{L_n^2 p^2}{4 A} + pL_n \quad (13)$$

### III. RESULTS AND DISCUSSION

To understand and explain the behavior of experimental data, it is first required to examine the dependence of the shunt resistance contribution,  $R_S/N$  due to dislocations in the base material as a function of the magnitude of space charge density,  $Q_{SC}$  around the core of a dislocation, the location of the trap levels contributing to the dislocation recombination and finally as a function of temperature. From Fig. 2 it is observed that the shunt resistance contribution due to dislocations is a steep function of  $Q_{SC}$  in a selected range of charges. At lower  $Q_{SC}$  the resistance is due to thermal generation of minority carriers and as tunneling current increases with the increase in  $Q_{SC}$ ,  $R_S/N$  is lowered and reaches a minimum. After the point where  $R_S/N$  is minimum, it is limited by surface recombination due to dislocation [12]. But from the top inset of Fig. 2 it is clear that it is not as strongly dependent on  $E_t$  as in HgCdTe [6]. Two trap energy levels for InGaSb, 0.1eV and 0.3eV above valence

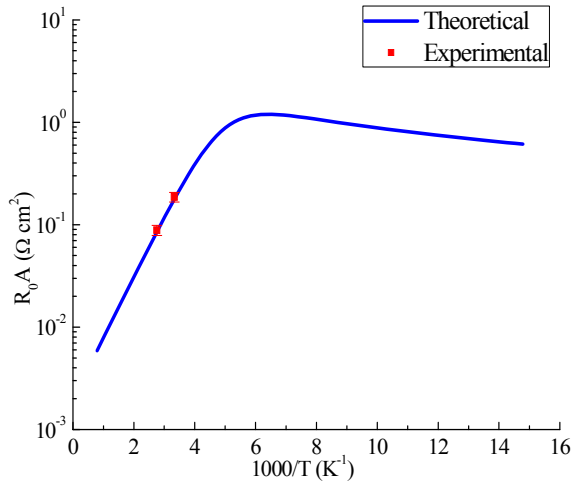


Figure 4. Zero-bias resistance-area product ( $R_0A$ ) as a function of temperature.

band  $E_v$ , is considered as reported in [13]. From Fig. 2 it can be seen that at sufficiently high temperature  $R_s/N$  increases.

#### A. Dislocation Effect on $R_0A$

The zero-bias resistance-area product as a function of dislocation is plotted in Fig. 3 using (8) for  $Q_{sc}/q = 1 \times 10^{25} \text{cm}^{-2}$ . From the figure it can be seen that experimental  $R_0A$  for  $40\mu\text{m}$  and  $100\mu\text{m}$  square diode fits well with the calculated curve and falls in the range of dislocation density  $(2.4 \pm 0.2) \times 10^8 \text{cm}^{-2}$ , reported from the measured data [9]. As can be seen, with the increase in dislocation density,  $R_0A$  reduces. This effect is theoretically predicted from (4) and (12) where increase in dislocation reduces the minority carrier lifetime as well as the shunt resistance contribution from surface leakage. This same effect has been observed for HgCdTe diodes in [4].

#### B. Temperature Effect on $R_0A$

Theoretically predicted  $R_0A$  variation with temperature using (8) is plotted in Fig. 4 for  $Q_{sc}/q = 1 \times 10^{25} \text{cm}^{-2}$  along with the two experimental data points. According to the calculation, for the present InGaSb photodiodes  $R_0A$  reaches a value of maximum  $1.85 \Omega \text{cm}^2$  at 139K. After that it continues reducing slightly from the maximum value. The reason behind such behavior of  $R_0A$  at low temperature can possibly be the lower  $E_g$  at these temperatures giving rise to a metallic property of the material. So there is scope for fitting experimental data at the low temperature region (less than 139K) for InGaSb PIN photodiodes.

### IV. CONCLUSIONS

InGaSb photodetectors working in the near infrared range find useful applications in various fields. These diodes are fabricated using metamorphic growth technology which results in dislocation in the base material. This initiates the necessity of taking dislocation density into account while characterizing them. In this paper, dislocation and temperature dependence of zero-bias resistance-area product of InGaSb is analyzed using a simple analytical model to calculate the impedance of individual line dislocations along the thickness of the wafer.

The model is based on the calculation of the dislocation dependence of minority carrier lifetime and recombination velocity of the carriers at the dislocations. The model fits well with the experimental data obtained for InGaSb PIN photodiodes at moderately high temperature of 300K and 363K and in dislocation density range of  $(2.4 \pm 0.2) \times 10^8 \text{cm}^{-2}$ . According to the model, the  $R_0A$  of InGaSb PIN photodiodes decrease after reaching a peak value of  $1.85 \Omega \text{cm}^2$  at 139K with the decrease in temperature. Assuming the dislocations to be uniformly distributed all over the sample, temperature and dislocation dependence of quantum efficiency and spectral response can also be satisfactorily modeled for InGaSb photodiodes.

#### ACKNOWLEDGMENT

Funding from the BUET's Research Office (CASR meeting no 218, agenda 97, dated 6 June 2009) is greatly acknowledged.

#### REFERENCES

- [1] P. S. Dutta, H. L. Bhat, and V. Kumar, "The physics and technology of gallium antimonide: An emerging optoelectronic material," J. Appl. Phys. vol. 81, pp. 5821-5870, May 1997.
- [2] S. M. Johnson, D. R. Rhiger, J. P. Rosebeck, J. M. Peterson, S. M. Taylor, and M. E. Boyd, "Effect of dislocations on the electrical and optical properties of long-wavelength infrared HgCdTe photovoltaic detectors," J. Vac. Sci. Technol., vol. 10(2), pp. 1499-1506, July 1992.
- [3] K. Jowikowski and A. Rogalski, "Effect of dislocations on performance of LWIR HgCdTe photodiodes," J. Electron. Mater., vol. 29, pp. 736-741, 2000.
- [4] V. Gopal and S. Gupta, "Effect of dislocations on the zero-bias resistance-area product, quantum efficiency, and spectral response of LWIR HgCdTe photovoltaic detectors," IEEE Trans. Electron. Devices, vol. 50, no. 5, pp. 1220-1226, May 2003.
- [5] V. Gopal and S. Gupta, "Contribution of dislocations to the zero-bias resistance-area product of LWIR HgCdTe photodiodes at low temperatures," IEEE Trans. Electron. Devices, vol. 51 (7), pp. 1220-1226, July 2004.
- [6] V. Bhagwat, Y. Xiao, I. Bhat, P. Dutta, T. F. Refaat, M. N. Abedin and V. Kumar, "Analysis of leakage currents in MOCVD grown GaInAsSb based photodetectors operating at  $2\mu\text{m}$ ," J. Electron. Mater., vol. 35, no. 8, pp. 1613-1617, April 2006.
- [7] J. A. González-Cuevas, T. F. Refaat, M. N. Abedin, and H. E. Elsayed-Ali, "Modeling of the temperature-dependent spectral response of  $\text{In}_{1-x}\text{Ga}_x\text{Sb}$  infrared photodetectors," Optical Engineering, vol. 45, no. 4, pp. 044001-1-044001-8, April 2006.
- [8] F. M. Mohammedy, "Growth, fabrication and characterization of metamorphic InGaSb photodetectors for application in  $2.0 \mu\text{m}$  and beyond", PhD Thesis, Dept. of ECE, McMaster University, Canada.
- [9] F. M. Mohammedy, O. Hulko, B. J. Robinson, D. A. Thompson and M. J. Deen, "Effect of growth temperature on InGaSb metamorphic layers and the fabrication of InGaSb p-i-n diodes," J. Vac. Sci. Technol., vol. 26(2), pp. 636-642, March 2008.
- [10] M. Tanzid and F. M. Mohammedy, "Analysis of zero-bias resistance-area product for InGaSb PIN photodiodes," in Proc. ICECE2010, p406, in press.
- [11] V. Gopal, "A general relation between zero-bias resistance-area product and perimeter-to-area ratio of the diodes in variable-area diode test structures", Semicond. Sci. Technol., vol. 11, pp. 1070-1076, 1996.
- [12] R. K. Bhan and V. Gopal, "Analysis of surface leakage currents due to zener tunnelling in HgCdTe photovoltaic diodes," Semicond. Sci. Technol., vol. 9, pp. 289-297, December 1993.
- [13] W. E. Spicer, I. Lindau, P. Skeath, and C. Y. Su, "Unified defect model and beyond," J. Vac. Sci. Technol., vol. 17(5), Sept./October 1980.